Friulian Journal of Science **10.** 2008, 33-60

The Roman Thermae and the Patriarchal Basilica of Aquileia analyzed by modern techniques of surveying and representation

DOMENICO VISINTINI*

Abstract. The paper deals with the analysis of the Roman Thermae and of the Patriarchal Basilica of Aquileia by means of the modern techniques of laser scanning and photogrammetric surveying and of representation.
As a preliminary *Introduction*, the noteworthy history of Aquileia is just briefly recalled, as well as that of the Great Roman Thermae, nowadays an area of archaeological excavations, and of the Patriarchal Basilica, one of the most significant monuments of Italian Romanesque architecture.
The following *Materials and methods* chapter is focused, after the explanation of how laser scanning functions, then the various operative steps to automatically acquire independent clouds of millions of 3D points, transform them into a geo-referenced colour textured unique 3D surface, and represent it in many different digital views.
Then, in the *Results* the practical surveying and representation application of the two Aquileia sites is shown, mentioning the full automation of the data acquisition in the field and the impressiveness of the data processing and the digital representations carried out with dedicated software.
In the *Discussion*, the experience gained from the Aquileia cases and future projects are discussed, mainly concentrating on key-points of the level of automation attainable in the data processing.

Key words. Cultural heritage, laser scanning, photogrammetry, representation, automation.

[1] Department of Georesources & Territory, University of Udine, Udine, Italy.
E-mail: domenico.visintini@uniud.it

1. Introduction

1.1 The history of Aquileia in brief

Aquileia lies in the plain of Friuli not far from the lagoon of Grado, on the western bank the river Natissa, whose ancient name could have been *Aquilis*, from which the city got its name. Its historical, cultural and religious importance, and last but not least the its symbolic identity as the "Friuli' Mother", can only be briefly reported in this paper.

The story begins in 181 BC, when the Romans built a town-fortress at a strategic geographical position, intended as a defensive outpost against attacks from foreign armies, an operational base for raids against the Gauls, living in the Alpine ranges, and for attacks against the neighbouring Illyria, Dalmatia and Pannonia. About three thousand soldiers-settlers first inhabited the town; in the space of a few years, they were joined by an other four thousand. The centre of Roman Aquileia lies along the present day SR352 National Road and follows what was the old consular road (see Figure 1). The ancient *cardo maximum*, now Via Giulia Augusta, runs right north-south through the city as far as the crossroads with the *decumanum maximum*, now Via Gemina, where we find the remains of the *Forum* (see ③ in Figure 1), in truth built later in II-III century, in particular the Eastern portico visible today.

In 89 BC, the colony became a *Municipium*. Later, under the rule of the Emperor Augustus it became capital of the "Venetia et Histria" Region X (the tenth Roman Region): along with this increased stature, the number of monuments and splendid public buildings grew. The local craftsmen were master goldsmiths and also worked with glass and terracotta. The city housed very talented artists that worked with marble and stone to create mosaics of incredible beauty.

Unfortunately, Aquileia then suffered attacks by groups of barbarian infiltrators but, when Diocletianus was named Emperor, it returned to its former splendour as one of the greatest cities in the Roman Empire, the fourth of Italy after Rome, Milan and Capua, and the ninth of the whole empire. A strong Christian community grew and drew upon the Apostles' preaching. The conversion to Christianity of Istria and the Balkans, Hungary at its territories as far as the Danube had its roots here. The sheer size of the areas concerned made Aquileia one of the major Christian sites and its status was added to considerably when the Bishop was endowed with the title of Patriarch.

Such glory and wealth however also invited more attacks. Attila, King of the Huns, arrived in 452 and, after a protracted siege, overcame the city defences and destroyed "everything in front of him". The population fled to Grado and to the islands around the lagoon that were easier to defend in the event of attack up to reach very far islands: in this way Venice was founded.

In the VI century with the Longobard invasion and the foundation of a new kingdom, Forum Julii (nowadays Cividale) became a dukedom and Aquileia lost some of its traditional

political and administrative power over the Region and the Patriarchs abandoned it.

Aquileia flourished once more thanks to Charlemagne who supported the return of Patriarch Massenzio. From the beginning of the IX century and throughout the X and XI centuries, Aquileia was restored to its original splendour. From 1077, the Emperor bestowed the power of feudal lord upon the Patriarch including the right to mint coin.

This Patriarchal dominion lasted for some centuries but the ever-increasing power of the Republic of Venice was to put an end to Patriarchal rule in 1420. From this time on, Aquileia slipped into a slow decline returning to its origins as a farming village.

In 1751, the diocese was finally abolished and the dismembered territories were assimilated into the Archbishopric of Udine, which had authority over the lands of Venice and Gorizia, with power over the Austrian territories.

To conclude this brief historical outline and to stress again the importance of Aquileia, it is sufficient to remember that, as is known, the Archaeological Area and the Basilica of Aquileia have been enrolled in the World Heritage List of the UNESCO during the XXII Session in Kyoto on 1998, thanks to the criteria III, IV and VI:

– Criterion III: Aquileia was one of the largest and most wealthy cities of the Early Roman Empire.
– Criterion IV: By virtue of the fact that most of ancient Aquileia survives intact and unexcavated, it is the most complete example of an Early Roman city in the Mediterranean world.
– Criterion VI: The Patriarchal Basilica complex in Aquileia played a decisive role in the spread of Christianity into central Europe in the early Middle Ages.

1.2 The Roman Thermae of Aquileia. The discovery by Giovanni Brusino of the Great Roman Thermae, spread over an area of perhaps two hectares in the western part of Aquileia (see ① in Figure 1), dates back to the years 1922-1923. New excavations were undertaken in 1961 by Luisa Bertacchi to prevent the construction of a school complex on the archaeological site and Paola Lopreato conducted more systematic surveys between 1981 and 1987. From 2002, the southern part of the spas constitutes the school field of archaeological investigations (see Figure 2 at left) of the University of Udine within the Degree course in Conservation of the Cultural Heritages (Fales et al. 2003).

The excavations, although partial, showed a north-south oriented wide rectangular area of about 140 x 30 m, which includes a large central hall of 47 x 20 m with a marble marquetry floor (*opus sectile*) and two rectangular, symmetric rooms of 30 x 20 m, decorated with rich polychrome, geometric mosaics. The style and quality is similar to the best examples in other regions of the Empire. These halls, linked by corridors and surrounded by tanks, were part of the *Frigidarium*, since there is not any trace of heating systems.

The refinement of the flooring, using marble tiles and tassels, glass paste, precious stones, such as porphyry and serpentine, confirms the exceptional importance of the spa complex of Aquileia, which must have been one of the largest of the Roman Empire. Many restorations of the mosaics show that the life of the Great Thermae was rather long, with several periods and various renovations, starting at least from the III century AD to continue in the fourth and, probably, even after this time.

Some of the beautiful mosaics of the Great Thermae have been recovered from the digs and are preserved in the Archaeological Museum of Aquileia (see ④ in Figure 1).

1.3 The Patriarchal Basilica of Aquileia. In the southeastern area of the Roman town (see ② in Figure 1), the Romanesque-Gothic lines of the Patriarchal Basilica rise stately and solemnly; in truth, its origins date back to the beginning of the IV century.

According to tradition, St. Mark brought the message of the Gospel to these lands, being sent here by St. Peter. As an Evangelist, during his mission in Aquileia, he met and converted Ermacora who became the first priest of the small Christian community. He was martyred with his deacon Fortunato, and they are, together with the Virgin Mary, the patron Saints of the Basilica. The persecution ended in 313 as a result of the Edict of Costantine and Licio. The Christian community of Aquileia, ruled by Archbishop Theodore, was then finally able to build its first church. In about one thousand years from that time, many architectural changes took place, so turning the Theodorian church into today is Basilica. The chronological evolution of the Basilica plan is reported in Visintini, Crosilla and Sepic (2006).

The first church was made up of two large rectangular halls: they were parallel to each other and connected by a third hall, that was later flanked by smaller rooms.

The Theodorian building was radically changed in the IV century: the north hall was hugely enlarged, in order to contain a greatly increasing number of faithful. After that, also the Theodorian south hall was transformed in a three aisled building (Post-Theodorian south hall) with a new great baptistery in front of its main entrance.

Attila destroyed the Post-Theodorian north hall during the siege in 452 and it was never rebuilt again.

In the IX century, the Patriarch Massenzio undertook a definitive restoration by constructing the transept which formed a cross shaped plan for the first time and the crypt under the presbytery. Then he adjusted the facade building the porch linking it to the Basilica through the so-called "Pagan' Church".

In the XI century, the Patriarch Poppone wanted to carry out further restoration. He built the perimeter walls, made a new roof, and the main apse was painted with frescoes of great monumentality of Roman inspiration. Poppone also built the 73 m high bell tower that dominates the

plain of Friuli. The present day Basilica (see Figure 2 at right) appears to the visitor practically as Poppone consecrated it in 1031 on July 13th.

In the XII century, the Patriarch Voldorico of Treffen embellished the crypt with a series of frescoes, one of the most important Romanic paintings in northern Italy.

Patriarch Marquardo from Randek completed a Gothic renovation after the 1348 earthquake, erecting ogival arcs in the nave and a wood roof with a trilobated keel shape.

Then, from the Middle Ages to the XIX century further additions of lesser importance were made to the Basilica.

Last but not least, the treasure both of art and faith and the most precious of the Basilica: the mosaic floor (e.g. Iacumin 1993, Marini 2003). It is the widest and oldest floor in the Christian western world, a magnificent example of Constantine Art. It is quite impressive that this masterpiece was only discovered in the 1909 by Austrian archaeologists under the pavement built by Poppone! The mosaic is made up of ten carpets separated by strips with *girali* (wreaths) of shoots and leaves of Acanthus. It can be defined as a "catechism through images", as each image has relevance, liveliness, imagination and the truth of faith, those truths that, in the 313, could finally be proclaimed in public.

2. Materials and methods. For a detailed analysis of important, extended, and complex monuments such as the Roman Thermae and the Patriarchal Basilica, the best available modern techniques for surveying and representation should be employed. A *Terrestrial Laser Scanner* (TLS) system integrated with a photogrammetric camera surely represents the *State-of-the-Art* surveying technique. The extraordinary amount of geometrical and imaging data automatically acquired by these devices, after the necessary processing steps, can be skilfully represented in many top-quality ways thanks to the never-ending development in the fields of 3D modelling and rendering, virtual reality, and computer vision.

The modern techniques of "surveying and representation" constitute the themes of this paper; nevertheless, since top-quality surveying is a necessary (and nowadays still sufficient) condition to get top-quality representations, attention is mainly focused on surveying topics. In this chapter *Materials and methods*, the different sections deal with the surveying technology used ("materials") and with the steps of the data processing ("methods"), including in the latter representation issues too.

2.1 Laser scanning and photogrammetric techniques of surveying. In order to fix the ideas, the similar definitions "terrestrial *laser scanner*" and "terrestrial *laser scanning*", both corresponding to the TLS acronym, have a different meaning: the *scanner* is the instrument ("material") allowing the surveying by *scanning* ("method"), although roughly speaking the concepts are analogous.

The first prototypes of TLS systems were put on the market less than

ten years ago (see e.g. Boehler, Heinz & Marbs 2002). At the beginning, they were employed for industrial and civil engineering investigations, while nowadays they are largely used for the surveying of architectural, archaeological and cultural heritage sites, where their geometric irregularity can be precisely measured with a high level of detail (see e.g. Sacerdote & Tucci 2007).

Figure 3 on the left shows the principle of measurements of the TLS surveying. The coordinate reference frame X^S, Y^S, Z^S has its origin in the TLS system centre and is defined as "Scanner' Own Coordinate System" (SOCS). The direction of the Z^S -axis can be approximately vertical only or can be turned, as in Figure 3, to scan almost horizontal surfaces such as an archaeological excavation area. Therefore, a SOCS is a local and arbitrary reference frame and this will require the computations described in paragraph 2.3.

In any case, let us consider emitting a laser beam in a certain spatial direction: the three coordinates of the strike point P are computed by applying the equations:

$$\begin{aligned} X^S &= D \sin\varphi \sin\vartheta \\ Y^S &= D \sin\varphi \cos\vartheta \\ Z^S &= D \cos\varphi \end{aligned} \qquad (1)$$

where:

– D is the distance from the TLS instrument to the point P: it is computed, as for a topographic EDM (Electronic Distance Meter), by the *time-of-flight* or *phase difference* methods exploiting the known form of the emitted-returned wave;
– φ is the "vertical" angle of the ray direction: it is known since it is imposed by the rotation of a mirror around the "horizontal" axis;
– ϑ is the "horizontal" angle of the ray direction: also this is known since it is imposed by the rotation of a mirror around the "vertical" Z^S-axis.

From the mathematical point of view, equations (1) express the (biunivocal) transformation from spherical coordinates D, φ, ϑ to Cartesian coordinates X^S, Y^S, Z^S.

Coming back to the TLS surveying, the *scanning* effect is achieved quickly (up to 50.000 times per second!) sending the laser beam in different directions by changing the mirror deflection angle by small increments. For each point, the value of D is measured, while those of φ and ϑ are imposed: by continuously applying equations (1), the corresponding X^S, Y^S, Z^S coordinates are then automatically computed in quasi *real-time*. High-accuracy in measuring the angular values is truly important, since the precision of the obtained X^S, Y^S, Z^S coordinate point depends on it: in general, the error in the point 3D positioning is restricted to a few millimetres.

Furthermore, also the intensity I of the returned laser signal is acquired, mapping in this way the various materials of the surface, that can be represented in a grey scale as in Figure 3, right.

Some TLS instruments can also measure the returned intensity in the

spectral band of the RGB (Red, Green and Blue) fundamental colours, so directly providing a *coloured cloud of points*, namely giving out seven values X^S, Y^S, Z^S, *I, R, G, B* for each point.

Instead most of the TLS systems do not work in the colour spectrum, but can be integrated with a high-resolution photogrammetric camera by firmly mounting this latter over its head (see Figure 3 at left). The system becomes a "laser scanner and photogrammetric integrated system", furnishing clouds of X^S, Y^S, Z^S, *I* points and digital metric images as those reported in Figure 2.

Using a photogrammetric camera, its centre of shot defines a new coordinate reference frame, called the "Camera Coordinate System" (CMCS), but whose rotation and translation from the SOCS origin are known, since the camera is rigidly mounted on the TLS system: this allows a fully automatic integration between laser scanning and imaging data, as will be shown in paragraph 2.6.

2.2 Laser scanning and photogrammetric data acquisition. The only manual operation to carry out in the field of surveying is the positioning of suitable cylindrical or adhesive flat reflecting targets, making the function of analytical "tie points" in dealing with different scans and consequently with different SOCSs, as will be described in paragraph 2.3.

The data acquisition is fully automatic and it is performed by setting the integrated system on a tripod in suitable fixed positions (stations), as for a topographic EDM. In spite of this, most kinds of TLS have neither the possibility of accurately setting vertical the principal axis, or an efficient centring mechanism: hence, the position of the instrumental centre and the principal axis direction remain undefined. Once fixed the angular increments for φ and ϑ, and eventually chosen the minimum and maximum values of φ e ϑ within the instrumental operative field of scan, the acquisition of millions of points from each position is automatically carried out in a few minutes, also for panoramic scans, i.e. when ϑ ranges from 0° to 360°.

Regarding the reflecting targets, they are automatically detected among the point clouds still *in-situ* thanks to their very high reflectivity: for each one, also a fine scan of about 10.000 laser beams can be thus quickly performed, so as to accurately measure their barycentre position.

Then, the digital images are acquired by rotating the photogrammetric camera around the Z^S -axis by a suitable step of ϑ, so as to obtain a "horizontal" field of view covering the "horizontal" field of scan. The "vertical" overlap of the images on the scan is about 90% with wide-angle objectives, less with normal focal length lens. The number of images necessary to cover 360° depends on the angle of the objective used and the percentage value (10÷40%) of an angular overlap for security: with a 20 mm objective and a 40% overlap, fourteen images are needed to cover a panoramic scan.

For each image acquired, the posi-

tion and attitude of the CMCS origin with respect to the SOCS are easily computable from the value of the imposed angle ϑ.

2.3 Laser scanning data registration. As already mentioned, acquiring TLS data from different points of scanning, namely from different SOCS, gives rise the problem of merging such independent clouds of points. This fundamental problem is known as "registration" of the scans.

Considering Figure 4 left, the problem is that, applying equations (1) for the same point P, the coordinates X^{S1}, Y^{S1}, Z^{S1} with respect to $SOCS_1$ are obviously different from those of X^{S2}, Y^{S2}, Z^{S2} with respect to $SOCS_2$; furthermore, this fact is much more evident in dealing with further scans (SOCSs).

For that reason, the registration problem requires the a priori definition and assumption of another coordinate reference frame, unique for all the scans, called "Project Coordinate System" (PRCS), e.g. an already existing and barycentric coordinate system with a perfectly vertical Z^P-axis.

Considering again Figure 4 left for the sake of simplicity, although the PRCS could not correspond either to $SOCS_1$ or to $SOCS_2$, the analytical problem is described from the vector equation:

$$\begin{bmatrix} X^{S1} \\ Y^{S1} \\ Z^{S1} \end{bmatrix} = \begin{bmatrix} X^{S1}_{S2} \\ Y^{S1}_{S2} \\ Z^{S1}_{S2} \end{bmatrix} + R(\Omega, \Phi, K) \begin{bmatrix} X^{S2} \\ Y^{S2} \\ Z^{S2} \end{bmatrix} \quad (2)$$

where:

- X^{S1}, Y^{S1}, Z^{S1} are the P coordinates with respect to PRCS (X^P, Y^P, Z^P);
- X^{S1}_{S2}, Y^{S1}_{S2}, Z^{S1}_{S2} are the unknown $SOCS_2$ origin coordinates with respect to $SOCS_1$, in fact with respect to PRCS (X^P_{S2}, Y^P_{S2}, Z^P_{S2});
- $\boldsymbol{R}$ is the matrix of the unknown rotation from $SOCS_2$ to $SOCS_1$ (in fact to PRCS), defined from three rotation angles Ω, Φ, K around three principal directions, called Euler' angles (or the analogous Cardan' angles).

As usual in geodetic sciences, the six unknowns are computed by creating a system with a redundant number of equations (2) over the same unknowns and by performing the so-called "least squares estimation", namely an optimal solution from the statistical point of view. This is done by exploiting the X^{S1}, Y^{S1}, Z^{S1} and X^{S2}, Y^{S2}, Z^{S2} "double" coordinates of at least two points (e.g. point A and point B), that is the same (e.g. A and B) points in the two scans, for this reason called "double points" or "tie points".

In principle, in the overlapping zone between two clouds there are millions of quasi common points, and so there are theoretically millions of double points to analytically solve the registration, but with the titanic problem of the correct pairing of the "same" points (the scanned point never is exactly the same in the different scans). All these troubles can be completely skipped by exploiting the reflecting targets as tie points, considering their barycentric SOCS coordinates, and automatically finding the correct point pairing by

choosing, among all the possible combinations, the one giving the minimum error (sum of the squares of the residuals).

Following the same approach for each couple of scans and/or considering the common targets among more than two scans, three translation and three rotation parameters per scan are computed. By applying these transformations to each point of each cloud, they "move" from their SOCS frame to a common PRCS frame: as a consequence, a unique cloud of millions of points is finally obtained.

2.4 Laser scanning data geo-referencing. After the registration, another topographic problem arises: the obtained unique PRCS point cloud should be referred to a "Global Coordinate System" (GLCS), e.g. a cartographic reference frame, hence requiring the so-called "geo-referencing" of the laser scanning data.

The problem of transforming X^P, Y^P, Z^P coordinates into X^G, Y^G, Z^G ones can be analytically solved by means of *direct* or *indirect* methods of geo-referencing (e.g. Schuhmacher & Böhm 2005).

In the former case, the TLS system is integrated with a GPS receiver and/or topographic devices so can be directly measured the transformation parameters from the various SOCS to GLCS frame, hence bypassing the registration step.

Following instead indirect methods, an interesting solution is possible if a large scale digital 3D cartography of the surveyed area is available: having found "double points", a sort of registration of the point cloud onto the digital cartography is therefore performed. Nevertheless, the most employed method follows the typical topographic approach: some scanned points (e.g. the same reflecting targets) constitute a set of "control points" surveyed by means of an EDM total station from several vertexes of a topographic network defined in a geodetic *datum*. Nowadays, the novelty in this approach is given by fixing the geodetic *datum* of the network by GPS measurements directly, instead of the indirect method of classical topographic measurements in regard to fiducial points in the surroundings belonging to some geodetic/cartographic network.

From the analytical point of view, the problem is described from a relationship very similar to the previous (2):

$$\begin{bmatrix} X^G \\ Y^G \\ Z^G \end{bmatrix} = \begin{bmatrix} X_P^G \\ Y_P^G \\ Z_P^G \end{bmatrix} + R(\Theta) \begin{bmatrix} X^P \\ Y^P \\ Z^P \end{bmatrix} \qquad (3)$$

where:

– X_P^G, Y_P^G, Z_P^G are the unknown PRCS origin coordinates with respect to GLCS;
– $\boldsymbol{R}$ is the matrix of the unknown rotation from PRCS to GLCS, defined from only one rotation angle Θ since Z^P-axis and Z^G-axis are both vertical.

Considering relationship (3), the least squares estimation of the unknowns follows the same strategy of the previous registration step § 2.3, where

now the double points are given from the control points, with topographically measured X^G, Y^G, Z^G coordinates and registered X^P, Y^P, Z^P ones.

Summarizing, from the analytical point of view, scan registration and scan geo-referencing both involve the estimation of translation and rotation parameters: for this reason, they can also be simultaneously solved. Furthermore, these TLS topics are analogous to the classic photogrammetric problems of the *relative orientation* between two images with the creation of a *stereoscopic model* (registration) and *absolute orientation* of the so-created stereoscopic model (geo-referencing).

2.5 Surface reconstruction from laser scanning points. The successive processing steps regard the removing of blunders and useless points and, above all, the conversion from a 3D point cloud to a 3D surface.

For the first goal, available software provide several commands and tools, implementing statistical analysis and/or geometrical criteria, to remove gross errors, *outliers* data, isolated points, duplicated points, and so on. In this way, it is possible to automatically "clean" and "filter" the point cloud, and to resample the scans by means of a less resolution angular grid, if this could be useful. Furthermore, classical CAD tools for manual 3D selection (and deletion) are always available.

The second aim instead concerns the creation (*modeling*) of the surface fitting the correct points, called "Dense Digital Surface Model" (DDSM) for its general very high resolution. From the geometrical point of view, the DDSM is a *finite elements* reconstruction by means of a surface function f_1 so that $S = f_1 (X^P, Y^P, Z^P)$; without loss of generality, given a certain X^P, Y^P "planimetric" value, S allows the Z^P "elevation" value, to be computed namely a function f_2 exists so that $Z^P = f_2 (X^P, Y^P)$.

In practice, the DDSM is automatically reconstructed by means of TIN (Triangulated Irregular Network) 3D meshes, best known as *Delaunay triangulations*, or by means of regular grids, namely a matrix of square cells, each one composed of two isosceles rectangular triangles. Afterwards, the obtained DDSM is generally submitted to a procedure of *smoothing*, averaging the small surface irregularities, and to a procedure of *decimation*, deleting and simplifying the much too small triangles (see for details e.g. Visintini 2007).

2.6 Integration with photogrammetric images. As told before, a TLS and photogrammetric system acquires digital images: for each one of these, the position and attitude of the CMCS origin with respect to the SOCS is easily computable from the corresponding imposed angle ϑ. Laser scan and imaging data can be thus integrated in a straightforward way, without the need for user manual interactions.

Considering in fact the following fundamental photogrammetric "equations of collinearity" for one acquired image, unlike what happens for classic photogrammetric problems, all the quantities on the right of the equal are known:

$$x = -c\frac{R_{11}(X^S - X_C^S) + R_{12}(Y^S - Y_C^S) + R_{13}(Z^S - Z_C^S)}{R_{31}(X^S - X_C^S) + R_{32}(Y^S - Y_C^S) + R_{33}(Z^S - Z_C^S)} + x_0$$
$$y = -c\frac{R_{21}(X^S - X_C^S) + R_{22}(Y^S - Y_C^S) + R_{23}(Z^S - Z_C^S)}{R_{31}(X^S - X_C^S) + R_{32}(Y^S - Y_C^S) + R_{33}(Z^S - Z_C^S)} + y_0 \quad (4)$$

where:
- x, y image (pixel) coordinates of a generic point depicted on the photogrammetric digital image;
- c, x_0, y_0 parameters of inner orientation of the camera, known from the process of photogrammetric calibration;
- X^S, Y^S, Z^S position of the same generic point, known since computed by equations (1) in the scanning process;
- R_{11}, R_{12},..., R_{33} matrix coefficients of the rotation from CMCS to SOCS, known since the camera is firmly fixed on the TLS top and it rotates by imposed ϑ angles;
- X_S^C, Y_S^C, Z_S^C translation from CMCS to SOCS, known since the camera is firmly fixed on the TLS top.

In greater detail, six parameters defining the initial rotation (involving three Euler angles) and translation from CMCS to SOCS called "mounting parameters" are known from a process of calibration of the TLS and the photogrammetric integrated system. When the camera rotates for the image acquisition, only the direction ϑ angle varies from one shot to another. The corresponding rotation matrix $\boldsymbol{R}$ and the translation vector X_S^C, Y_S^C, Z_S^C are easily computed.

For each point, equations (4) express the central projection joining together the SOCS 3D coordinate X^S, Y^S, Z^S and the corresponding CMCS 2D (image) coordinates x, y. The RGB values relating to such pixels are then used to "color" the point. Repeating the same operation for all the points depicted in one image, the point cloud become a colored point cloud, as can be seen in Figure 4 on the right.

Afterwards the procedure of colouring is carried out for all the images acquired from each scan position: this process takes only a few seconds and can be done during the field operations. As one can note, the 3D/2D integration is performed in the SOCS frame: however, by means of the scan registration and geo-referencing, the coloured point clouds "move" from SOCS frames to GLCS frame.

This laser scanning and imaging integration allows also the fully automatic colour texturing (*wrapping*) of the DDSM with the RGB values: from the analytical point of view, for such projection, equations (4) are applied considering the laser point coordinates as X^S, Y^S, Z^S values, but the X^P, Y^P, f_2 (X^P, Y^P) coordinates of the surface.

Last but not least automatic product is the "orthophoto", namely a geometrically correct (orthogonal) image displaced onto a plane of interest, e.g. horizontal or vertical. Either

the orientation of the digital image or the object surface $S = f_1 (X^P, Y^P, Z^P)$ must be know: both are known in laser scanning and photogrammetric integrated surveying. In order to obtain the orthophoto image, equations (4) are thus exploited again for the digital resampling required. Some software project the textured 3D DDSM onto the 2D plane, involved while others project the original 2D image onto the 2D plane, taking into account the different values $X^P = f_2 (X^P, Y^P)$ from the DDSM.

2.7 Digital representations of the surveying. The concept of "representation" is now enucleated, starting of the assumption to skilfully exploiting the extraordinary capability of modern software for realistically rendering, virtual reality, and computer vision. Once a detailed 3D model textured with image colours has been obtained, as seen before, the production of an infinite number of different "2D digital representations" is automatically done just in real-time! The user has rather to decide on the "what, how, and from where" to represent! Examples of the resulting representations for the Aquileia sites surveying are shown and described throughout chapter 3 (*Results*).

Answering in inverse order the triple dilemma, "from where" query involves the basic projective geometry concept of the view point position: a finite distance from the object to represent yields a perspective view (e.g. Figure 6 and Figure 13), while an infinite distance generates an orthogonal view. In the latter case, when the representation planes are coplanar with two PRCS or GLCS axes, the views constitute the six so-called "Monge' representations", best known as (nadiral) *plan* (from the top) (e.g. Figure 8 and Figure 16), *zenithal plan* (from the bottom), forward, backward, left, and right *prospect*. To obtain each of these, the user has to simply "press the corresponding button" to! When such Monge' representations are printed in a certain conventional scale, they correspond to the classical *plotting sheets* widely used for civil engineering and architecture purposes.

By picking a point in the view, generally with the left mouse button, and moving the mouse, every rotation of the representation plane is possible and the corresponding perspective or orthogonal view is provided in real time! As is well-known, considering the intersection of the DDSM with a vertical plane having a certain azimuthal direction, the corresponding vector section is automatically obtained; nevertheless, by selecting a "strip" of points between two close parallel planes, a "pseudo-section" can be also produced. At last, when the DDSM or all the points over one plane are considered, a unified vector section and *raster* prospect is automatically achieved (e.g. Figure 7 and Figure 15).

The "how to represent" question concerns the way to represent laser photogrammetric surveying, since many graphic tools are available. The point cloud can be coloured, with different dot sizes and with or without smoothing techniques in the visualization, by grey scale according to the

intensity I value (e.g. Figure 3 right), or by false colours according to the distance from the PRCS or to the Z^P elevation, or by true RGB colours. The DDSM meshes can be represented (e.g. Figure 6 and Figure 14) in a transparent form by *wireframe* vectors, or in a solid form by 3D faces with flatted or smoothed colours or textured with RGB images, and with or without a wireframe overlay. A DDSM with RGB textured faces without a wireframe overlay is the more realistic photo representation of the surface the surveyed object.

Last but not least, "what to represent" means one can choose, for the output view, all or only some parts of the surveyed object, as well as other geo-referenced data such as 3D vector digital cartography, 2D aerial orthophotos, and also paper maps after their digitalization and appropriate geo-referencing. Furthermore, the geometry of the object in the past, as reported in historical maps (e.g. Figure 18 at left) or virtually reconstructed (e.g. Figure 9), at the present and in the future, as planned by a restoration project, can be mixed together in the same 3D model. In brief, the user is free to exploit the geometrical 3D data acquired and available, for a more complete analyses of the object of interest.

Concluding the remarks on the extraordinary potential of present day representations, two last points concern the dynamic representations and the link with thematic databases. The first goal is fulfilled within immersive virtual environments, e.g. the VRML (Virtual Reality Modeling Language) space or the Google Earth one, by means of interactive movements (explorations) or along predefined trajectories (navigations) such as AVI video files with possible multimedia effects. For the second scope, once geometrical data have been suitably linked to the descriptive data by means of DBMS (Database Management System) software, each single object can be interrogated by just clicking onto it, as a simplified query of a Geographical Information System (GIS). For instance, both possibilities have been carried out for the 3D model of the Victoria Square of Gorizia obtained from aerial and terrestrial laser scanning and photogrammetric surveying (see for details Visintini, Spangher & Fico 2007).

3. Results. For surveying the Roman Thermae and the Patriarchal Basilica, the Riegl Z360I Austrian laser system (http://www.riegl.com) integrated with a Nikon D100 photogrammetric digital camera (http://www.nikon-imaging.com) of the Laboratory of Photogrammetry of the University of Venice was employed. The main results obtained by means of the RiSCAN PRO® (Riegl) software, are briefly described throughout this chapter.

3.1 Laser scanning and photogrammetric surveying of the Roman Thermae. The southern part of the spas ("Scavo Lopreato") was surveyed during the excavations in summer 2005: at the beginning, 33 cylindrical (5 cm diameter x 5 cm height) reflecting targets were placed in the area.

The acquisition step § 2.2 of data belonging to a quasi-horizontal surface as an archaeological area is, requires turning the TLS Z^S -axis in tens of degrees and, if possible, lifting the point of scanning. For this reason, a suitable scaffold was placed close to the "Aula Sud" to elevate the TLS about 5 m above the ground (see Figure 5 left and Figure 2 left). A 35° pointing downwards scan was thus carried out, with an angular resolution of 0,030° so acquiring a cloud of 6,7 millions points! Furthermore, from the same high position, a panoramic vertical scan of the surroundings within a radius of about 200 m was performed. Nevertheless, two other scans were carried out from the western boundary of the digs, one vertical and one turned at 40° (see Figure 3), and so about 23 million points were collected overall.

From the same four scan stations, a total number of 64 high-resolution (3.008 x 2.000 pixel) digital images were acquired with a 20 mm focal length objective, with a mean carefulness overlap of 40%.

Simultaneously, the 33 reflecting targets were topographically surveyed with a Leica TCRA 1103 EDM station from two vertexes. From these latter, other reference points were also measured, in particular the steel pickets driven into the ground to form a 5 m square grid and used by the archaeologists to geo-reference the measurements of *direct surveying* of the excavations. In this way, by means of the so-called "inverse intersection" topographic scheme it was later possible to compute the position of the two vertexes in the same reference frame adopted by the archaeologists, so constituting the PRCS of the TLS surveying. Therefore, the coordinates of the reflecting targets and, as a consequence, whose of the registered scans refer to the same PRCS; the cartographic geo-referencing § 2.4, not of primary interest for the work, was not carried out. All the surveying operations in the spas area were performed in half a day.

The step § 2.3 of registration of the four scans was easily carried out, thanks to the fact that, for TLS acquisitions in the open field, all 33 targets are practically visible in each scan and so the six unknown per scan of equations (2) can be solved by a very redundant system. The numerical statistical values obtained by RiSCAN PRO elaborations confirm this optimal operative condition: the barycentre position of the cylindrical targets after the registration differ on average by only 5 mm. In this way, an overall cloud of 23 million points was achieved, with a mean density in the "Aula Sud" zone of 30.000 points per square meter, that is one 3D point every 5,8 mm!

For the successive step § 2.5 of DDSM reconstruction, within RiSCAN PRO software, various procedures are available for irregular and regular 3D modeling. For an archaeological quasi-horizontal area, the 3D modeling based on a 2D regular grid promises the best results with respect to the TIN approach. Considering therefore a planimetric grid with a step of 5 x 5 cm along Z^P and Y^P directions, the corresponding Z^P value

of about 200.000 vertexes constituting the DDSM of the year 2005 excavations (see Figure 6) have been automatically computed.

As can be seen in this perspective view, the DDSM, reconstructed by very small isosceles rectangular triangles and represented in a smoothed shaded form, looks like a continuous surface: its false colour, from red to blue, are according to the height.

3.2 Representations of the Roman Thermae. By suitably exploiting the RiSCAN PRO tools, a large number of 2D/3D numerical products such as sections, profiles and raster/vector mixed representations have been automatically obtained for the archaeological area.

Vertical sections every 10 cm of the DDSM were generated at once: 453 along X^P transversal direction and 143 along Y^P longitudinal direction, one of those is reported in Figure 7 as well as the part of the spas beyond the section towards the east, as an example of combined section/prospect.

Moreover, horizontal sections every 1 cm gave 41 *contour lines* reported in Figure 8, as an example of raster/vector mixed planimetric representation, together with the orthophoto on the horizontal plane, result of the integration step § 2.6 with the Nikon photogrammetric images.

Starting from a detailed 3D model like this (Figure 9 left) and thanks to archaeological knowledge and historical hypothesis (Rubinich 2006), it has been possible to virtually rebuilt the Roman Thermae as they were (Figure 9 right). These reconstructions are nowadays very popular in documentaries on history and archaeology, often truly spectacular from the cinematographic point of view: the likelihood of such reconstructions strongly depends on the completeness of the 3D geometrical surveying and the correctness of the constructive hypothesis.

3.3 Laser scanning and photogrammetric surveying of the Patriarchal Basilica. The acquisition of laser scanning and photogrammetric data with the Riegl Z360I integrated with a Nikon D100 camera and the processing with RiSCAN PRO software for the surveying of Patriarchal Basilica are similar to those relating to the Roman Thermae.

On the other hand, an internal and fully 3D space, with many columns, other visual obstacles and occluded parts, very much complicates the surveying operations: many scans are required with strong variations in the scanning density, in the overlapping among the clouds, and in the distribution of the common targets.

The data were acquired in three days in December 2006. Initially 53 reflecting targets, cylinders (as for the spas) or adhesive circles (5 cm diameter), were placed inside and outside the Basilica as "tie points" for the steps of registration and geo-referencing. The laser instrument was therefore placed on a tripod at 13 suitable scan positions inside the Basilica. From these, 28 point clouds, with different Z^S -axis orientation, an-

gular steps and measured distance ranges, were collected. Anyway, from each instrument position, a panoramic scan with the maximum instrumental angular resolution was accomplished, so acquiring a cloud of 3.240.000 points. For the quasi-vertical scan "AbsideV" of the Basilica main apse, acquired from a station practically in its centre, a 5 x 5 mm point grid, that is 40.000 points per square meter, on the frescoed wall surface were carried out! Figure 10 illustrates the panoramic scan "NavataV" executed from the centre of the central nave in an interesting 2D view in angular coordinates, namely each measured point is plotted in the ϑ, φ 2D space according to its angular acquisition values with respect to the SOCS.

From the same scan stations, a total number of 138 digital images were acquired with a variable factor of carefulness overlap: Figure 11 reports the twelve Nikon images of "NavataV" scan with its own overlap, so as to form a pseudo-panoramic image.

Figure 12 shows instead the result of the colouring step § 2.5 of the point cloud, again in a 2D view: as can be seen, the vertical field-of-view of the camera is smaller than the field-of-view of the TLS. The points of the ceiling and the floor not depicted in these images will be thus coloured in oblique scans with the corresponding images.

The external survey of the Basilica frontal part and of the 73 meters high bell tower was carried out from five stations, making possible 14 different scans, from a panoramic view of the surrounds to a very narrow of the bell tower only, and 55 digital images.

The 53 inside and outside one reflecting targets were suitably surveyed with a Leica TCRA 1103 EDM station from six vertexes of a topographic network. One Leica 520 GPS receiver was placed on one vertex (*master*), while a second equal GPS receiver (*rover*) on three other vertexes, so to perform *static differential satellite measurements*. This allowed as the network datum to be fixed directly into the Italian national Gauss-Boaga cartographic system assumed as GLCS. As a consequence, all the reflecting targets are referred to the GLCS: as a cascade consequence, the 13 inner scans and the 5 outer ones have been simultaneously registered and geo-referenced. Figure 13 shows a perspective view of the common cloud of about 55 million points obtained from the inner scans, each one with a different colour.

Twelve reflecting targets were on average exploited for each scan: the resulting mean residual is 2-3 cm and it is really satisfactory, above all considering the difficulty to topographically collimate the centre of the cylindrical targets.

As an example of the processing done on TLS and photogrammetric data, Figure 14 collects those carried out for the sixth left column (visible also in Figures 10÷12):

1. A part of the photogrammetric image depicting the column.
2. The cloud points of the column merged from the three closest TLS scans.
3. The DDSM of the column in the

form of very small TINs represented in wireframe.
4. The same DDSM represented by shaded gray-values according to TLS intensity.
5. The orthophoto prospect in the vertical plan from image 1. and DDSM 3.

Particular interest was focused on the superb mosaic floor: starting from about 3 million points acquired, the DDSM reconstruction step § 2.4 was carried out by exploiting the regular grid approach. Considering a step of 5 x 5 cm, the Z^P value of about 150.000 vertexes constituting the mosaic surface were automatically computed; this DDSM made it possible to produce the floor orthophoto of Figure 16.

What's more, aerial data were also employed, since an *Aerial Laser Scanning* (ALS) surveying with an Optech ALTM 3033 system for the whole town of Aquileia had been previously carried out, within the activities of the European Project INTERREG IIIA Italy-Slovenia (http://geomatica.uniud.it). The Research Group of Geomatics of the University of Udine has extensively tested the advanced and innovative ALS surveying technique for the city of Gorizia, also integrated with TLS data. The promising potentialities and results are described e.g. in Visintini, Crosilla, Fico and Guerra (2005). Coming back to the Aquileia ALS available data having a low density (1-2 points per square meter), since referred to the same Gauss-Boaga datum, a unique terrestrial and aerial point cloud was obtained at once! The representations of the results of the ALS data processing are reported in Figure 17, together with the TLS data.

Other details on the TLS surveying of the Basilica and the automatic modeling of the main apse can be found in Visintini, Crosilla and Sepic (2006).

3.4 Representations of the Patriarchal Basilica. Many digital representations of the Basilica have been automatically obtained with RiSCAN PRO, but only some are presented in this paragraph. Figure 15 reports a transversal section/prospect showing the good congruence among internal and external scans: by assigning a certain size to the points and using the smoothing option in the visualization, this point cloud already seems an orthophoto on a vertical plane.

Figure 16 is instead a raster/vector plan of the mosaic floor produced by means of a real orthophoto from the Nikon images, where one pixel corresponds to one cm, together with one centimeter contour lines, showing its strong irregularity due to the ground subsidence.

The 3D coloured model of the Basilica has been exported in various file formats, so allowing very realistic virtual visits, either in VRML environment or along outside or inside tours in AVI multimedia file. One virtual navigation movie can be seen at low resolution, together with other ALS and TLS surveying examples, at the web page http://geomatica.uniud.it/progetti/laserscan/.

Another example of virtual trajectory, this one approaching the Basilica, is depicted throughout Figure 17,

in order to represent all together ALS, TLS, and photogrammetric data. The figures, are more understandable in Visintini (2007), show in the order:

1. ALS points coloured by elevation (from blue to red).
2. ALS points automatically classified in "ground" (brown) and in "non ground" (white).
3. ALS "non ground" points automatically classified in "buildings" (red) and in "vegetation" (green).
4. Shaded buildings models semi-automatically obtained from "buildings" points.
5. Wire-frame buildings models and TLS RGB coloured points.

6.7. TLS RGB coloured points and textured DDSM of the mosaic floor.

8.9. Textured DDSM of the mosaic floor.

These different views have to be considered as single "frames" from which to construct a virtual navigation in the inner or outer space and/or in the time, with more or less impressive "cinematographic special effects".

Last but not least, Figure 18 shows two other examples of achieved virtual representations. On the left, the present-day Basilica with the pavement covering the mosaics as reported in a plan by Niemann in 1909, before being removed. On the right, the area of the Basilica with the buildings modelled and texturized as a *3D City Model* with a *Level of Detail* 3 (e.g. Visintini, Spangher & Fico 2007) imported as a KMZ file inside the well-known virtual geographical space of Google Earth.

Discussion. This paper describes the application of the modern techniques of surveying and representation for the analysis of the Roman Thermae and the Patriarchal Basilica of Aquileia, both belonging to the World Heritage List of the UNESCO.

The importance of these two monuments, briefly recalled here, could be sufficient to give a good reason for the use of State-of-the-Art surveying and representation techniques; nevertheless, the complexity of these Aquileia sites clearly demonstrate the ability of these extraordinary modern "materials and methods".

An excursus within the terrestrial surveying by means of laser scanning systems integrated with a photogrammetric camera has been employed, as well as in the processing steps of data registration, geo-referencing, surface reconstruction and imaging integration. We can say that this technology has truthfully revolutionized the geo-topo-cartographic world and that we are only at the beginning in exploiting its huge potential for architectural and engineering disciplines relating to territory, urban planning, building construction, and cultural heritage sectors.

Its key feature is the acquisition of an abnormal number of geometric and photographic information, which no other surveying technique has never been able to offer. Data processing becomes the key stage of the process, also since there is nothing to do dur-

ing the fully automatic data acquisition! With a metaphorical expression, this technique challenges the talented surveyor to be able to bring the astonishing level of automation of the data acquisition into the data processing.

The interested reader should now ask the fundamental question: "How automatic were the surveying and the representations for Aquileia Thermae and Basilica?". Remembering again the fully-automatic data acquisition in only three-four days, the level of automation really accomplished in the processing can be quoted as fully-automatic again for the steps of surface reconstruction, of imaging integration, and of course of digital representations, this latter taking advantage of the present-day wonderful resources of computer sciences. The steps of registration and geo-referencing were carried out in a "quasi-automatic" way: simply renaming the target points exactly as the control points skips any trouble, otherwise, permutation algorithms find the correct coupling well enough. Hence, we can state that the available software solve automatically also these processing steps.

Concluding, throughout the Aquileia experience, such surveying and representation techniques have been evaluated in real applicative cases on two different but nonetheless complex monuments such as an archaeological open area and an enclosed space of a Romanesque-Gothic church, obtaining positive responses in both cases.

The realistic likelihood of the produced digital representations here presented can surely be improved by other editing and refinement steps, but every elaboration so added removes the representation process from a "press the button" process, as instead is the aim of the challenge in which we are involved.

Finally, the fundamental question must arise again, now in the form "How good are the results gained in a fully automatic way?" There is not an all-season answer to it since a lot, if not everything, depends to the software managing the laser scanning and photogrammetric data. Consequently, we are (alas) in the hands of computer scientists and programmers implementing more or less complex algorithms, whose performances are today generally more than satisfactory.

Anyway, to conclude on an optimistic note and trusting in inexorable technological developments, we can await in near future astonishing results even for all the processing considered very complex up to now or (nearly!) impossible!

Figure 1. Ortofotografie aerie di Aquilee cun la indicazion des Grandis Termis Romanis ①, de Basiliche Patriarcjâl ②, dal Fori Roman ③ e dal Museu Archeologjic ④. / Figure 1. Aerial orthophoto of Aquileia with indication of the Great Roman Thermae ①, the Patriarchal Basilica ②, the Roman Forum ③, and the Archaeological Museum ④.

Figure 2. Lis Grandis Termis Romanis (a çampe) e la Basiliche Patriarcjâl (a diestre) di Aquilee in dôs imagjins metrichis cjapadis sù cun la cjamare dal sisteme integrât laser scanner e fotogrametric. / Figure 2. The Great Roman Thermae (left) and the Patriarchal Basilica (right) of Aquileia in two metric images acquired by the camera of the laser scanner and photogrammetric integrated system.

Figure 3. Il sisteme laser scanner e fotogrametric dilunc la acuisizion dai dâts intes Termis Romanis (a çampe) e il nûl di ponts 3D misurâts e colorâts secont la intensitât tornade indaûr al strument (a diestre). / Figure 3. The laser scanner and photogrammetric system during the data acquisition in the Roman Thermae (left) and the cloud of the measured 3D points coloured by the returned intensity (right).

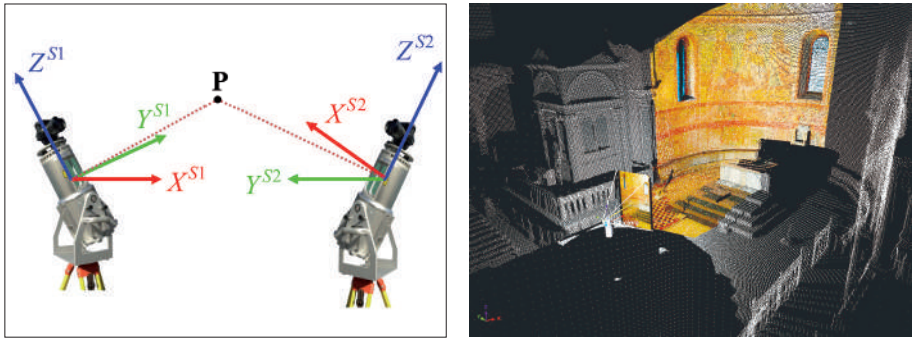

Figure 4. Principi de regjistrazion (a çampe): di diferentis coordenadis SOCS a unichis coordenadis PRCS. Principi de colorazion dal nûl di ponts (a diestre): proiezion dai valôrs RGB di une imagjin digjitâl. / Figure 4. Principle of the registration (left): from different SOCS coordinates to unique PRCS ones. Principle of colouring of the point cloud (right): projection of the RGB values from a digital image.

Figure 5. Acuisizion dai dâts midiant Riegl Z360I di une impalcadure inte aree sud des Termis Romanis (a çampe). Une imagjin digjitâl de "Aule Sud" cjapade sù cun la cjamare metriche Nikon D100 (a diestre). / Figure 5. Data acquisition with Riegl Z360I from a scaffold in the Roman Thermae southern area (left). One digital image of the "Aula Sud" so acquired with the Nikon D100 photogrammetric camera (right).

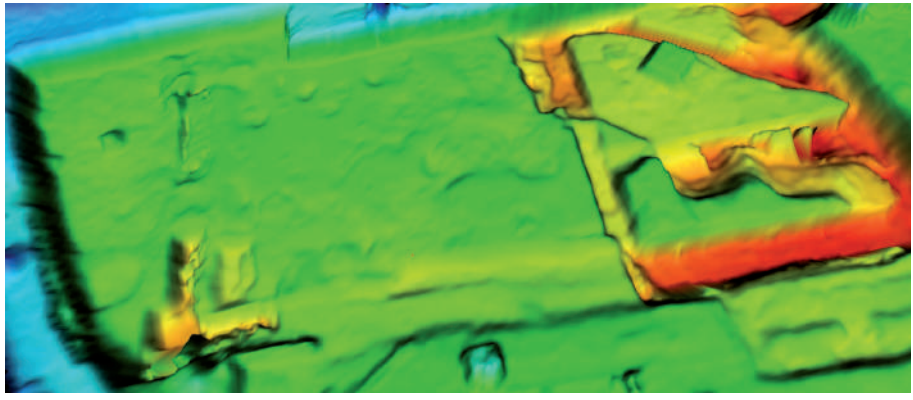

Figure 6. La superficie sfumade dai sgjâfs archeologjics des Termis Romanis colorade par altece. / Figure 6. The shaded surface of the archaeological digs of the Roman Thermae coloured by height.

Figure 7. Sezion/prospet longjitudinâl dai sgjâfs archeologjics des Termis Romanis, cun viste viers Est. / Figure 7. Longitudinal section/prospect of the archaeological digs of the Roman Thermae with view towards East.

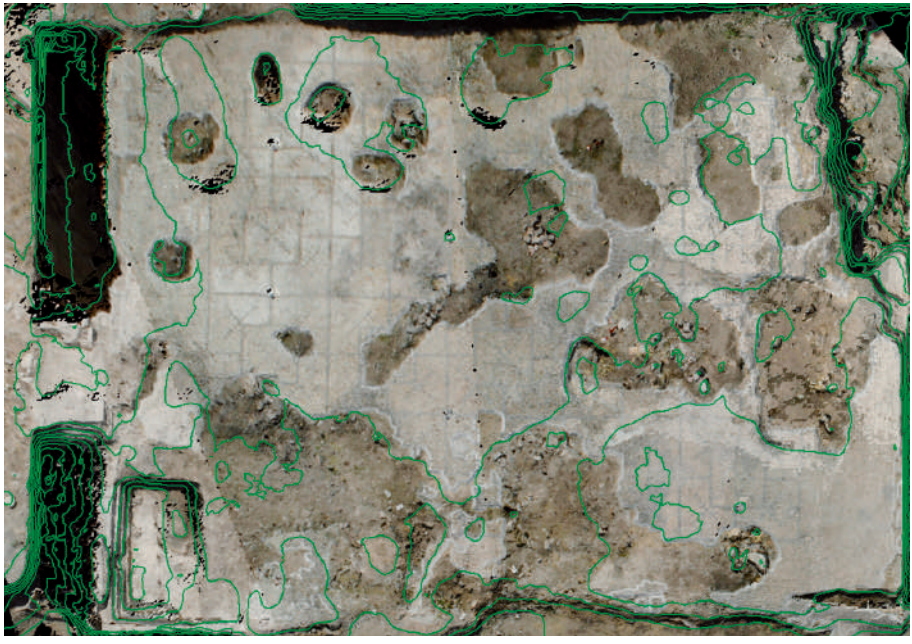

Figure 8. Ortofoto e curvis di livel ogni centimetri dai sgjâfs archeologjics des Termis Romanis. / Figure 8. Orthophoto and 1 cm contour lines of the archaeological digs of the Roman Thermae.

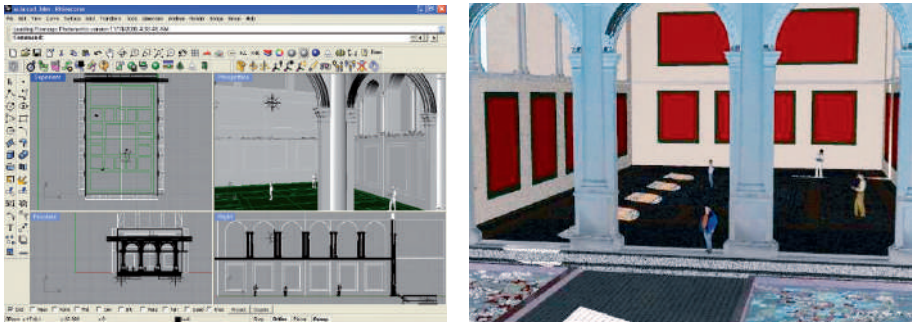

Figure 9. Dal model 3D rilevât a la ricostruzion virtuâl des Termis Romanis (Rubinich 2006). / Figure 9. From the surveyed 3D model to the virtual reconstruction of Roman Thermae (Rubinich 2006).

Figure 10. Viodude 2D in coordenadis angolârs de scansion panoramiche "NavataV" colorade par intensitât. / Figure 10. 2D view in angular coordinates of the panoramic scan "NavataV" coloured by intensity.

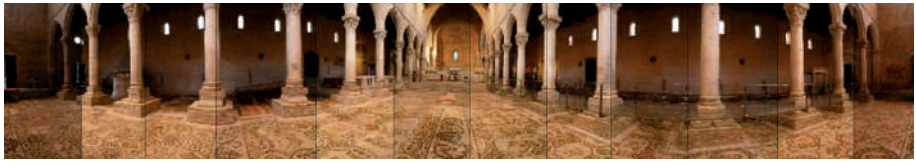

Figure 11. Imagjin pseudo-panoramiche otignude cun lis 12 imagjins a colôrs de scansion "NavataV". / Figure 11. Pseudo-panoramic image obtained by the 12 overlapped colour images of "NavataV" scan.

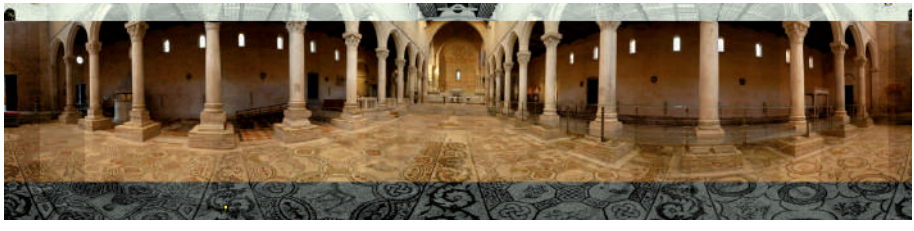

Figure 12. Viodude angolâr 2D de scansion "NavataV" colorade dai valôrs RGB des imagjins digjitâls. / Figure 12. 2D angular view of scan "NavataV" coloured by RGB values from the digital images.

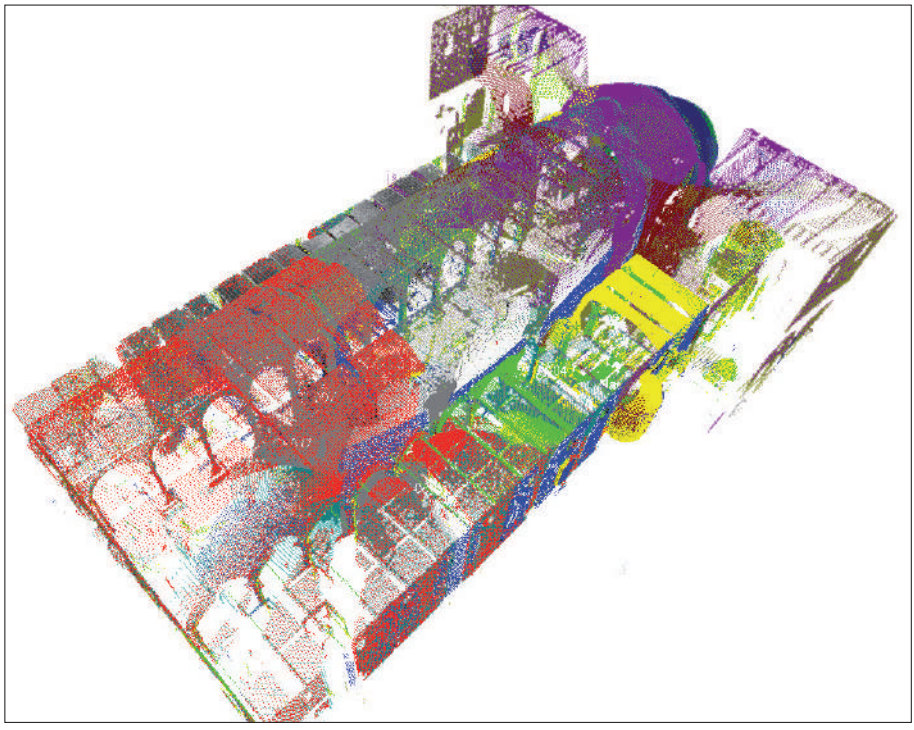

Figure 13. Lis 13 scansions internis in colôrs diferents dopo la regjistrazion e la gjeo-referenziazion. / Figure 13. The 13 inner scans in different colours after simultaneous registration and geo-referencing.

Figure 14. Une colone de Basiliche (a çampe): dal nûl di ponts TLS al prospet midiant ortofoto (a diestre). / Figure 14. One Basilica column (at left): from the cloud of points to the prospect by orthophoto (at right).

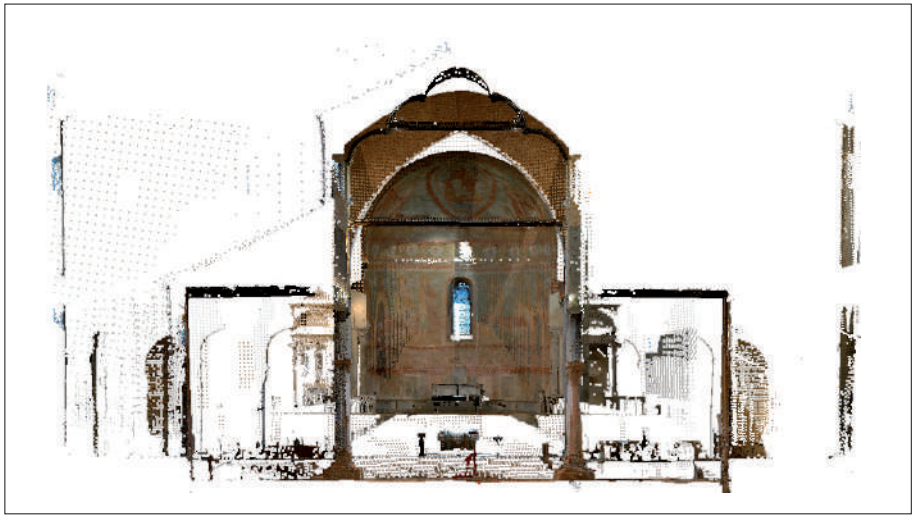

Figure 15. Prospet/sezion trasversâl de Basiliche cun viodude viers la abside. / Figure 15. Transversal section/prospect of the Basilica towards the apse.

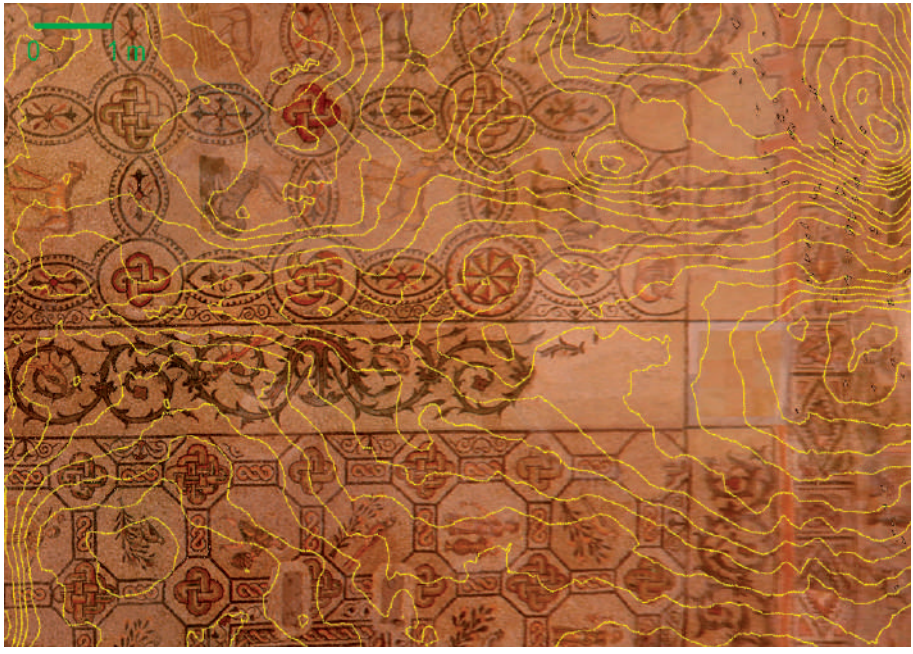

Figure 16. Plante dal magnific paviment a mosaic de Basiliche midiant ortofoto e curvis di livel ogni cm. / Figure 16. Plan of the magnificent mosaic floor of the Basilica by orthophoto and 1 cm contour lines.

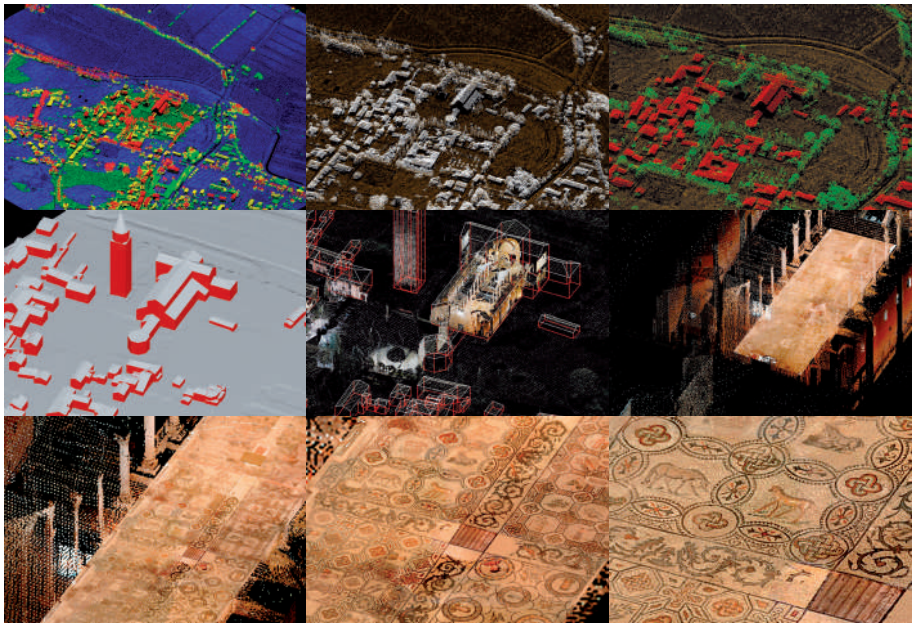

Figure 17. Viodudis assonometrichis rivant fin te Basiliche fra dâts laser scanning aeris e terestris. / Figure 17. Axonometric views approaching the Basilica among aerial and terrestrial laser scanning data.

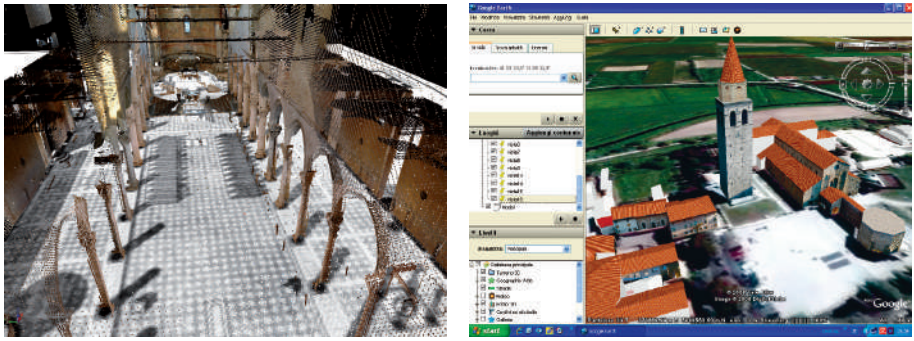

Figure 18. La Basiliche cul paviment dal 1909 (a çampe) e dentri dal spazi di Google Earth (a diestre). / Figure 18. The Basilica with the 1909 floor (left) and inside the Google Earth virtual space (right).

Bibliografie/ References

Boehler W., Heinz G., Marbs A. (2002). The potential of non-contact close range laser scanners for cultural heritage recording. In *International Archives of Photogrammetry, Remote Sensing and Spatial Information Sciences. Proceedings of the XVIIIth International Symposium of CIPA, Potsdam*, XXXIV, 5/C7, pp. 430-436.

Fales M.F., Maselli Scotti F., Rubinich M., Clementi T., Magnani S., Rebaudo L., Saccocci A., Sperti L. (2003). Università di Udine. Aquileia: scavi dell'edificio pubblico detto "delle Grandi Terme" – Campagne 2002-2003. *Aquileia Nostra*, LXXIV: 181-287.

Iacumin R. (1993). *La Basilica di Aquileia*. II: *Il mosaico dell'Aula Teodoriana*. Reana del Rojale (Ud): Chiandetti Editore.

Marini G. (ed.) (2003). *I mosaici della Basilica di Aquileia.* Fondazione Società per la Conservazione della Basilica di Aquileia. Villanova del Ghebbo (Ro): CISCRA Edizioni.

Rubinich M. (2006). Le indagini dell'Università di Udine alle "Grandi Terme" di Aquileia, loc. Braida Murada (scavi 2005-2006). *Notiziario della Soprintendenza per i Beni Archeologici del Friuli Venezia Giulia*, 1: 151-158.

Sacerdote F., Tucci G. (eds.) (2007). *Sistemi a scansione per l'Architettura e il Territorio.* Firenze: Alinea Editrice.

Schuhmacher S., Böhm J. (2005). Georeferencing of terrestrial laserscanner data for applications in architectural modelling. *International Archives of Photogrammetry, Remote Sensing and Spatial Information Sciences*, *Proceedings of the ISPRS Working Group V/4 Workshop 3D-ARCH 2005, Mestre-Venezia*, XXXVI, 5/W17 (on CD).

Visintini D. (2007). Interpretazione, modellazione e prodotti finali. In Sacerdote F., Tucci G. (eds.) *Sistemi a scansione per l'Architettura e il Territorio.* Firenze: Alinea Editrice, pp. 57-85.

Visintini D., Crosilla F., Fico B., Guerra F. (2005). A 3D virtual model of the Gorizia downtown (Italy) by matching aerial and terrestrial surveying techniques. In *International Archives of Photogrammetry, Remote Sensing and Spatial Information Sciences. Proceedings of the XIXth International Symposium of CIPA, Torino, IAPRS*, XXXVI, 5/C34, 1: 575-580.

Visintini D., Crosilla F., Sepic F. (2006). Laser scanning survey of the Aquileia Basilica (Italy) and automatic modeling of the volumetric primitives. *International Archives of Photogrammetry, Remote Sensing and Spatial Information Sciences*, *Proceedings of the ISPRS Commission V Symposium, Dresden*, XXXVI, 5 (on CD).

Visintini D., Spangher A., Fico B. (2007). The VRML model of Victoria Square in Gorizia (Italy) from laser scanning and photogrammetric 3D surveys. *Proceedings of the Web3D 2007 Symposium – 12th International Conference on 3D Web Technology*, *Perugia*, ACM SIGGRAPH: 165-168.